

Manifestation of quasiparticle branch imbalance in resistive measurements of mesoscopic superconductors

K. Yu. Arutyunov

Low Temperature Department, Physics Faculty, Moscow State University, Moscow 119899, Russia

(Received 4 May 1995; revised manuscript received 13 October 1995)

A model of the resistive state for mesoscopic superconductors has been proposed. It is considered that the frequency of thermally induced discrete phase-slip events is equal to the rate of thermally driven fluctuations, Γ_T . After each phase slippage the nonequilibrium distribution of chemical potentials for pairs μ_p and quasiparticles μ_q relaxes on a time scale τ_{Q^*} . The measured time-averaged voltage across the mesoscopic sample with dimensions compared to a single phase-slip center is found to be proportional to the spatial difference of the corresponding chemical potential (μ_p for superconducting probes and μ_q for normal probes) and should be multiplied by the time averaging weight $\sim \tau_{Q^*}\Gamma_T$. The resulting effective resistance ratio $\langle R(T) \rangle / R_{\text{normal}}$ for mesoscopic objects may be noticeably greater than unity sufficiently close to the critical temperature; it displays a strong nonlinear dependence on the bias current and is greatly suppressed by an external magnetic field.

I. INTRODUCTION

The dimensionality of a superconducting sample is determined by the relation of geometrical dimensions to the coherence length ξ . If external magnetic field or bias current is applied, then the field penetration length λ should be also taken into consideration. As both quantities diverge at a critical temperature T_c , formally each sample of finite dimensions could be considered as zero dimensional (0D) close enough to T_c . However, to study a conventional type-I superconductor in a 1D mesoscopic regime [transverse dimensions less than and length comparable to $\xi(T)$] in an experimentally controllable range of temperatures one should take a micrometer-length sample.

At the present moment contactless galvanomagnetic measurements of a single mesoscopic sample lie beyond experimental capabilities. The easiest way to study electronic transport is the conventional four-probe method. However, one should always keep in mind that on a mesoscopic scale quantum interference plays an essential role. The existence of electrodes may significantly change the properties of the whole system "sample with electrodes" in comparison with the solitary mesoscopic original.

It should be also emphasized that the properties of a superconductor in a resistive state dramatically differ from purely superconducting or normal conditions. It was found^{1,2} that for homogeneous steady-state injection of quasiparticles the chemical potentials of pairs μ_p and quasiparticles μ_q differ from each other. The models describing the resistive state of 1D superconductors induced by thermal fluctuations^{3,4} or bias current⁵ involve the conception of phase slippage which is a process of rapid oscillations of the order parameter Δ within the locus of the "weak link." For pulselike pumping of nonequilibrium quasiparticles due to discrete activation of phase-slip (PS) centers the actual values of $\mu_{p,q}$ are determined by the temporal and spatial dependences of corresponding relaxation processes. The behavior of a PS center could be described by the model of a

simple transmission line, so that charge imbalance waves may propagate in the 1D superconductor in analogy with electrical signals that propagate down the transmission line.⁶ The corresponding decay length Λ depends on material properties, temperature, and the frequency of PS "pumping."

Recent experiments on mesoscopic Al samples⁷⁻¹⁰ have revealed several anomalies of the resistive state of such small objects. The resistive transition displays a "bump" on top of the $R(T)$ dependence. The amplitude of this bump is greatly influenced by the value of the bias current and external magnetic field. The anomaly totally disappears for samples longer than several micrometers.⁷

Here we present a model which describes the behavior of a 1D mesoscopic sample in the resistive state. We consider the nonequilibrium charge imbalance to be maintained by thermally activated PS events. PSs are pumped with a frequency Γ_T equal to the rate of thermally induced fluctuations and relax on a time scale τ_{Q^*} . We assume the mesoscopic wire to be sufficiently short so that only one PS center at a time could enter the sample. The time-averaged voltage across the sample is considered to be proportional to the difference of the instantaneous values "just after" the PS event of corresponding chemical potentials [μ_p for superconducting (S) probes and μ_q for normal (N) probes¹¹] multiplied by the time-averaging "weight" $\tau_{Q^*}\Gamma_T$. The resulting effective resistance ratio $\langle R \rangle / R_{\text{normal}}$ displays strong nonlinear behavior on a bias current, is efficiently suppressed by an external magnetic field, and is always smaller than unity for samples longer than several zero-temperature coherence lengths ξ_0 (Table I).

II. THEORY

Let us consider a superconducting mesoscopic 1D wire [Fig. 1(a)] in a resistive state close to the critical temperature T_c . The destruction of superconductivity can be described by the model of thermally induced fluctuations.³ Each "fluctuation event" is nothing more than the PS which drives the

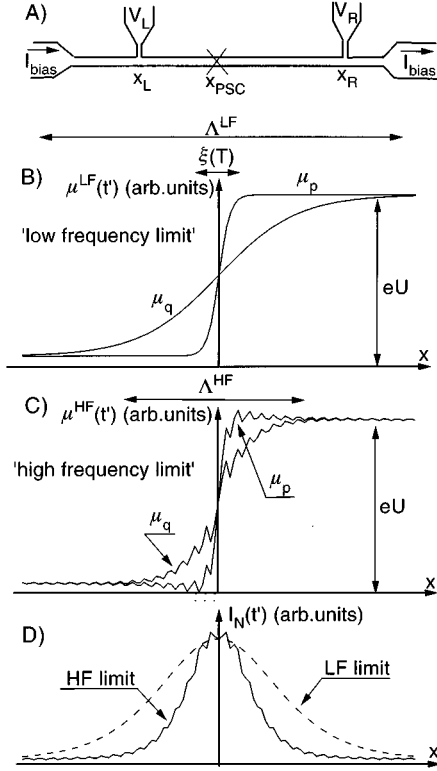


FIG. 1. (a) Sketch of the sample. (b),(c) Spatial dependences of the instantaneous values of chemical potentials for pairs μ_p and quasiparticles μ_q at a moment t' just after the phase-slip event for the low-frequency and the high-frequency limits, respectively. (d) Corresponding spatial dependences for the instant values of the normal-current component.

system from one local minimum of the free energy F'_{\min} to another one F''_{\min} which differs by the phase value $\varphi' - \varphi'' = \pm 2\pi$ of the complex order parameter $\Delta(\varphi)$. It was shown^{3,4} that the rate of thermal fluctuations, Γ_T , at a bias current I is

$$\Gamma_T(T, I) = \Omega(T) \exp \left[-\frac{\Delta F_0}{k_B T} - \left(\frac{2}{3} \right)^{1/2} \frac{I^2}{3\pi I_1 I_c} \right] \sinh \left(\frac{I}{2I_1} \right). \quad (1)$$

The prefactor $\Omega(T)$ is equal to

$$\Omega(T) = \frac{1}{\tau_{GL}} \frac{L}{\xi(T)} \left(\frac{\Delta F_0}{k_B T} \right)^{1/2} \left(1 - \frac{2I}{3I_c} \right)^{15/4}, \quad (2)$$

where $\tau_{GL} = \pi\hbar/8k_B(T_c - T)$ is the characteristic gap relaxation time in the gapless limit. I_c is the temperature-dependent critical current.

The second and the third factors of Eq. (2) correspond to the number of statistically independent subsystems and overlapping of their fluctuations, respectively. As we consider a mesoscopic wire of length $L \sim \xi(T)$, then only one PS center could fit in the sample. Thus, hereafter we assume the second and the third factors of Eq. (2) equal to unity.

The ΔF_0 in the exponent of Eq. (1) is the free-energy barrier between the neighboring saddle points F'_{\min} and F''_{\min} in the zero-current limit. In the original work³ it was shown that

$$\Delta F_0 = \frac{8\sqrt{2}}{3} A (g_N - g_S) \xi(T), \quad (3)$$

where A is the sample cross section. The free energy advantage per unit volume enjoyed by the superconducting state relative to the normal state is

$$g_N - g_S = \frac{H_c^2(T)}{8\pi}. \quad (4)$$

However, in recent publications^{12,13} it was reported that for best fitting to experimental results on small objects the expression (3) for the energy barrier should be multiplied by a dimensionless factor $\gamma \sim 0.05$. The question of applicability of the ‘‘bulk’’ equations (3) and (4) to mesoscopic samples lies beyond the scope of the present work and needs further serious justification. Nevertheless, in the present work we assume that Eqs. (3), (4) hold with $\gamma = 1$. Note that very small variations of the critical temperature T_c could compensate the significant deviations of γ from unity.

The physical sense of the last term in Eq. (1) is the fact that the supercurrent I breaks symmetry between the PS $\varphi' - \varphi'' = \pm 2\pi$, driving fluctuations in the current-reducing direction. The characteristic threshold current is $I_1 = k_B T / \phi_0$, where ϕ_0 is the superconducting flux quantum. Thus, I_1 is a sample-independent quantity and is equal to ~ 25 nA which is not a small value for mesoscopic objects. The current-dependent terms in the exponent of Eq. (1) and Eq. (2) play a significant role for ‘‘high’’ values of $I/I_c(T) \sim 1$. As the critical current $I_c(T)$ tends to zero at T_c , the mentioned current dependencies must be taken into consideration for calculations close to the critical temperature. It should be emphasized that the basic assumption of the theoretical model³ is the hypothesis that the nucleation of resistivity in 1D superconductors is governed by very large and improbable fluctuations when $\Delta F_0 \gg k_B T$. Very close to T_c both the energy barrier ΔF_0 and the prefactor $\Omega(T)$ go to zero and the model³ does not work. Hereafter we consider that below some threshold temperature $T^* \sim \Delta F_0 / k_B$ the application of the fluctuation model is permitted.^{14,15} Note that the energy barrier ΔF_0 is dimension dependent and for mesoscopic samples it may shift the applicability of the model³ by several mK below T_c .

After each event of PS, driven at a frequency Γ_T equal to the rate of thermal fluctuations, there arises the quasiparticle branch imbalance Q^* , which relaxes on a time scale τ_{Q^*} and on a distance Λ . The relaxation of charge imbalance Q^* in a 1D superconducting wire can be described by the differential equation⁶

$$D \tau_{Q^*} \nabla^2 Q^* = \tau_0 \tau_E \ddot{Q}^* + (\tau_0 + \tau_E) \dot{Q}^* + Q^*, \quad (5)$$

where τ_E is the inelastic electron-phonon collision time, $\tau_0 = 2k_B T_c \hbar / \pi \Delta^2$ is the supercurrent response time, and $D = \frac{1}{3} v_F l$ is diffusion coefficient, v_F being the Fermi velocity

and l the electron mean free path. In the ‘‘low-frequency limit’’ Eq. (5) describes charge imbalance decay with the characteristic decay length

$$\Lambda^{\text{LF}} = (D\tau_{Q^*})^{1/2}. \quad (6)$$

In the ‘‘ultrahigh-frequency limit’’ $\omega \gg \tau_E^{-1}, \tau_0^{-1}$, Eq. (5) describes waves of charge imbalance, propagating with velocity $v = \Lambda/(\tau_0\tau_E)^{1/2}$. For the more general case where neither ultrahigh- nor low-frequency approximations are appropriate, Eq. (5) describes damped, dispersive waves of charge imbalance with the dispersion relation

$$-\Lambda^2 k^2 = (1 + i\omega\tau_0)(1 + i\omega\tau_E), \quad (7)$$

which decay on a length

$$\Lambda = \Lambda^{\text{LF}}(\tau_0\tau_E)^{1/2}/[\frac{1}{2}(\tau_0 + \tau_E)]. \quad (8)$$

As in the present paper we are discussing the thermal activation of charge imbalance, the characteristic frequency of the process ω is set by the rate Γ_T . For mesoscopic objects of conventional type-I superconductors the ultrahigh-frequency limit is never reached. However, the low-frequency $\Gamma_T \ll \tau_{Q^*}^{-1}$ or the high-frequency $\Gamma_T \gg \tau_{Q^*}^{-1}$ limits could be achieved.

If the PS event happens at $t = t_{\text{PS}}$, we may consider quasiparticles and pairs to be in a local equilibrium among themselves but not being in equilibrium with each other after a moment t' : $\tau_0 < \tau_E \leq t' - t_{\text{PS}} < \tau_{Q^*}$.² The local equilibrium approximation permits one to characterize quasiparticles and pairs by definite values of chemical potentials, which differ from their equilibrium value $\mu_q^{\text{stat}} = \mu_p^{\text{stat}} = \mu$. Following Ref. 16 let us approximate the low-frequency limit spatial variations of the instantaneous values of chemical potentials μ_p and μ_q at a moment t' by

$$\mu_p(t', x) = \frac{eU_p}{2} \tanh\left(\frac{x - x_{\text{PSC}}}{\xi/2}\right), \quad (9a)$$

$$\mu_q(t', x) = \frac{eU_q}{2} \tanh\left(\frac{x - x_{\text{PSC}}}{\Lambda}\right), \quad (9b)$$

where $\Lambda = \Lambda^{\text{LF}}$ and x_{PSC} is the coordinate of the PS center [Fig. 1(b)]. As μ_p and μ_q should merge into each other at $x = \pm\infty$ we may set $U_p = U_q = U$. For the high-frequency limit the ‘‘average’’ values of μ_p and μ_q could also be approximated by Eq. (9), while there exist the oscillations due to preceding PS events and, what is more important, the decay length $\Lambda = \Lambda^{\text{HF}}$ is shorter than the corresponding low-frequency value Λ^{LF} [Fig. 1(c)].

If not to discuss the processes on time scales less than the charge neutrality maintenance $\tau_{\text{CH}} \ll \tau_0, \tau_E, \tau_{Q^*}$, in the vicinity of the nonequilibrium region one may use the generalized two-fluid model to describe the electronic transport. At every moment t the total bias current could be split into two parts corresponding to pairs and quasiparticles $I(t) = I_S(t) + I_N(t)$. For the normal component of the current at a moment t' we may derive

$$I_N(t', x) = I - I_S(t', x) = -\frac{1}{e\rho_q(x)} \frac{d\mu_q(t')}{dx}, \quad (10)$$

where $\rho_q(x)$ is the effective resistance per unit length, associated with the quasiparticle current. Substituting (9) into (10) we get

$$I_N(t', x) = -\frac{U/2}{\Lambda\rho_q(x)} \cosh^{-2}\left(\frac{x - x_{\text{PSC}}}{\Lambda}\right), \quad (11)$$

a bell-shaped function localized at x_{PSC} [Fig. 1(d)]. Setting $x = x_{\text{PSC}}$ for the absolute value of $U = |U|$ we obtain

$$U = 2\Lambda\rho_q(x)[I - I_S(t', x_{\text{PSC}})]. \quad (12)$$

As we restrict ourselves to the moment t' ‘‘just after the PS event’’ we may assume that the total current is mainly carried by the quasiparticle excitations: $I \approx I_N(t', x_{\text{PSC}}) \gg I_S(t', x_{\text{PSC}})$. In the present paper we concentrate attention on mesoscopic length scales $\leq \Lambda$, which makes it possible to set the effective coordinate-dependent ‘‘quasiparticle resistance’’ equal to the corresponding value in normal state $\rho_q(x) \approx \rho_N = \text{const}$. Finally we get

$$U = 2\Lambda\rho_N I, \quad (13)$$

which gives the well-known result for the time-averaged voltage across the PS center, measured far away from the nonequilibrium region.¹⁶

It should be reemphasized that the nonequilibrium distribution (9) is maintained with frequency Γ_T and relaxes on a time scale τ_{Q^*} . We assume that the measured time-averaged voltage across the mesoscopic sample is proportional to the difference of the instantaneous values of corresponding chemical potentials, given by Eq. (9), and should be multiplied by the time-averaging weight $\sim \tau_{Q^*}\Gamma_T$,

$$\langle \Delta V_{p,q} \rangle = (\tau_{Q^*}\Gamma_T) \Delta\mu_{p,q}/e. \quad (14)$$

Introducing the normal state resistance $R_{\text{normal}} = \rho_N|x_L - x_R|$, where x_L and x_R are the coordinates of potential probes, for the effective ‘‘dynamic’’ resistance $\langle R \rangle = \langle \Delta V \rangle / I$ we get

$$\frac{\langle R \rangle}{R_{\text{normal}}} = (\tau_{Q^*}\Gamma_T) \frac{\Lambda}{|x_L - x_R|} \left[\tanh \frac{x_R - x_{\text{PSC}}}{\delta} - \tanh \frac{x_L - x_{\text{PSC}}}{\delta} \right], \quad (15)$$

where δ is equal to $\xi(T)/2$ for S probes and to Λ for N probes, which measure the difference between the corresponding values of chemical potentials μ_p and μ_q , respectively.⁶ Equation (15) is the central result of the present paper.

III. CALCULATIONS

Let us calculate the effective resistance ratio for various situations. The characteristic time of the charge imbalance relaxation τ_{Q^*} is given by¹⁷

$$\frac{1}{\tau_{Q^*}} = \frac{\pi\Delta}{4k_B T} \frac{1}{\tau_E} \left[1 + \frac{2\tau_E}{\tau_S} \right]^{1/2}, \quad (16)$$

where τ_S is the elastic pair-breaking time due to supercurrent or magnetic field, and in the most general case the gap parameter $\Delta = \Delta(T, I, H)$.

First, we discuss the situation when the external magnetic field is zero and the bias current I is small enough that we

TABLE I. Material parameters used in present calculations.

Material ^a	T_c (K)	$\tau_E(T_c)$ (10^{-8} s)	v_F (10^8 cm/s)	$H_c^{\text{bulk}}(0)$ (Oe)	l (nm)	λ_L (nm)	ξ_0 (nm)
Al	1.2	1.3	1.3	99	15	16	1600
Sn	3.73	0.027	0.7	306	15	35	230
Zn ^b	0.88	20	0.9	55	15	28	1800

^aData are taken from Refs. 5,20.

^bValues for zinc correspond to averaging the initially anisotropic data.

can neglect the corresponding pair breaking. Note that for the “true” zero-current limit $\Gamma_T=0$. For the case of negligible pair breaking the temperature dependence of $\tau_{Q^*}(T)$ is mainly determined by the variation of $\Delta(T)$ and the scale is set by the material-dependent parameter τ_E having no singularities at T_c . For conventional type-I superconductors of given dimensions, Γ_T varies within the same order due to “slight” differences of $H_c(0)$ and $\xi(0)$, while τ_E may vary significantly (Table I). The “short- τ_E ” materials (Sn, In, Pb) are always, even in case of significant pair breaking, in the low-frequency limit $\tau_{Q^*} \ll 1/\Gamma_T$. On the contrary, Zn could be generally considered in the high-frequency limit. However, the mesoscopic Al samples studied to date for practical bias currents are within the intermediate situation $\tau_{Q^*} \sim 1/\Gamma_T$. Thus, the material properties play a significant role in the behavior of the effective resistance ratio $\langle R \rangle / R_{\text{normal}}$ (Fig. 2). For simplicity hereafter we assume the weakest link (the midpoint of the PS center) to be located straight between the potential probes. Of course, for the real sample the weak link is pinned to the imperfection. However, the nonsymmetric placement of the PS center will reduce the magnitude of the resistive bump [see Eq. (15)], while all the calculations will stay qualitatively valid.

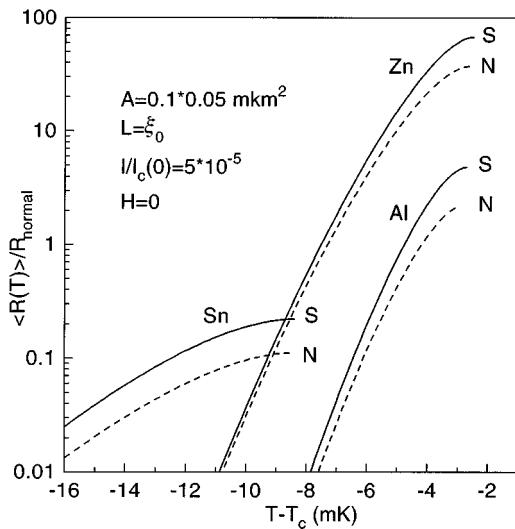


FIG. 2. Temperature dependences of the normalized effective resistance $\langle R \rangle / R_{\text{normal}}$ for tin, zinc, and aluminum samples of equal cross section A , effective length L/ξ_0 , and bias current $I/I_c(0)$ for zero magnetic field H . The signs S and N correspond to superconducting and normal potential probes, respectively. The PS center is assumed to be symmetrically referred to the voltage probes.

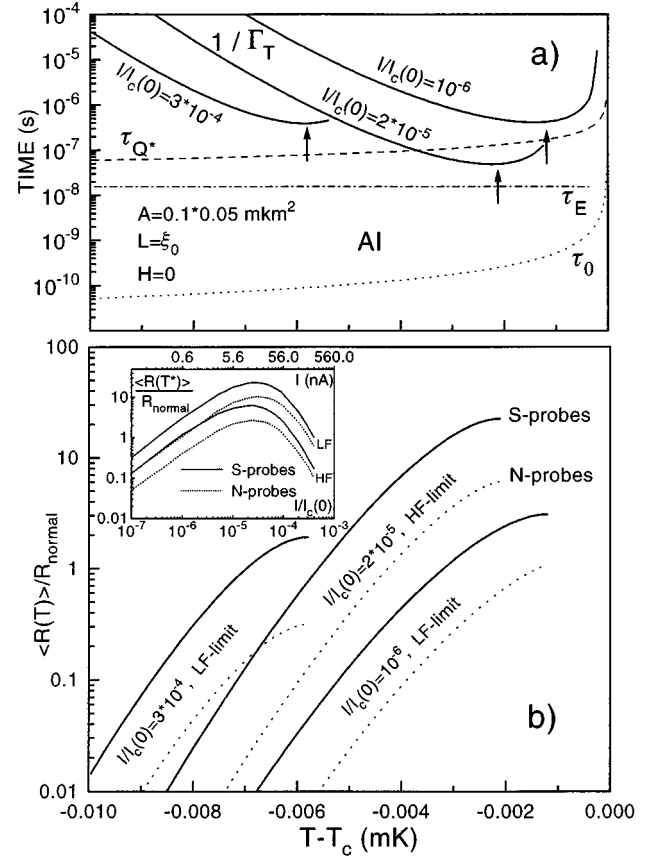


FIG. 3. (a) Temperature dependences of characteristic times for an aluminum sample with cross section A and length L at zero magnetic field H for different values of effective bias current $I/I_c(0)$. Arrows indicate the positions of the threshold temperature T^* . Note the evolution of the temperature dependences of the thermal fluctuation rate Γ_T with the bias current I . (b) The corresponding temperature dependences for the effective resistance ratio $\langle R \rangle / R_{\text{normal}}$ for symmetric position of the voltage probes referred to the PS center. The inset shows the variation of the maximum value of $\langle R \rangle / R_{\text{normal}}$, corresponding to $T = T^*$, with bias current I .

The pair breaking due to supercurrent may be taken into consideration by^{18,19} $1/\tau_S^I = D(p_S/\hbar)^2/2$, where p_S is the supercurrent momentum. Using familiar expressions²⁰ the τ_S^I could be rewritten in a more convenient form

$$\frac{1}{\tau_S^I} = \frac{D}{2} \left[\frac{I}{3\sqrt{3}I_c(T)\xi(T)} \right]^2. \quad (17)$$

Formally one has to consider the variation of the gap $\Delta = \Delta(I)$ with applied current.^{18,19} However, in the present paper we neglect this small $\Delta(I)$ deviation, which plays no significant quantitative role for calculations. Note that for high currents $I \sim I_c(T)$ one must consider the current dependence in the exponent of Eq. (1) and the prefactor $\Omega(T)$. The supercurrent I always brings the rate of thermal fluctuations, Γ_T , to higher values. Thus for aluminum structure (Fig. 3) for sufficiently small effective currents $I/I_c(0)$ the sample is in a low-frequency limit: The nonequilibrium quasiparticles can relax on a time scale τ_{Q^*} between successive fluctuation events ($\tau_{Q^*} < 1/\Gamma_T$) within the whole temperature region.

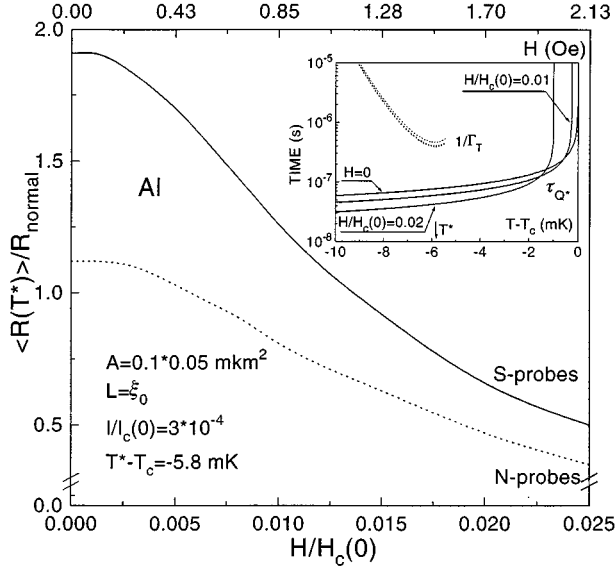


FIG. 4. Magnetic field $\vec{H} \parallel$ plane of the sample) dependence of the maximum value $\langle R \rangle / R_{\text{normal}}$, corresponding to $T = T^*$, for an aluminum sample with cross section A , fixed bias current I , length L , and symmetric position of the voltage probes referred to the PS center. The inset shows the influence of the magnetic field on temperature dependences of corresponding characteristic times: the period of thermal fluctuations $1/\Gamma_T$ and the quasiparticle relaxation time τ_{Q^*} . The arrow indicates the position of the threshold temperature T^* .

With increasing the bias current I very close to the critical temperature T_c the situation is shifted to the opposite limit, while for very strong currents there are no high-frequency solutions as the bias current I should not increase the temperature-dependent critical value $I_c(T)$.

The pair-breaking time for the case of a plain 1D wire in applied parallel magnetic field H is²²

$$\frac{1}{\tau_S^H} = \frac{1.76k_B T_c}{\hbar} \frac{H^2}{H_c^{\parallel}(0)}, \quad (18)$$

where $H_c^{\parallel}(0)$ is the zero-temperature parallel critical field. Contrary to the case of pair-breaking currents the variation of the gap with magnetic field^{20,22} $\Delta(T, H) = \Delta(T)[1 - H^2/H_c^{\parallel}(T)^2]^{1/2}$ plays a quantitatively significant role. Slightly affecting the $1/\Gamma$ due to variation of the gap $\Delta(H)$, the magnetic field noticeably shifts $\tau_{Q^*}(H)$ to shorter values, driving the sample to the low-frequency limit (Fig. 4).

For fixed temperatures within the resistive transition Eq. (15) gives negative effective magnetoresistance due to decreasing of $\tau_{Q^*}(H)$ [and, consequently, $\Lambda(H)$] with magnetic field. The above effect has been observed experimentally²³ and could partially describe the anomalous form of Little-Parks oscillations for mesoscopic loops.^{9,10}

The noticeable decreasing of effective resistance ratio $\langle R \rangle / R_{\text{normal}}$ with increasing the length of the sample, $L = |x_L - x_R|$, is due to $\sim \tanh(L)/L$ dependence of Eq. (15) (Fig. 5). The difference for N and S probes comes from different ‘‘healing’’ lengths Λ and $\xi/2$, respectively. Note

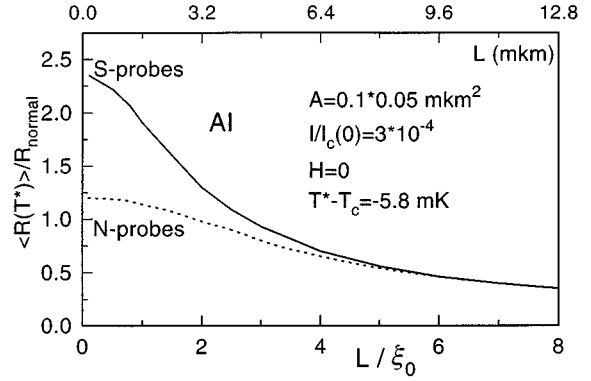


FIG. 5. Sample length $L = |x_L - x_R|$ dependences of the maximum value $\langle R \rangle / R_{\text{normal}}$, corresponding to $T = T^*$, for an aluminum sample with cross section A and symmetric position of the voltage probes referred to the PS center at fixed bias current I and zero magnetic field H .

that the present model could not be applied without modifications to long wires where more than one PS center could fit in the sample. Experimentally one can estimate the possible number of the active PS centers at a given temperature as being equal to the number of the voltage steps of the corresponding current-voltage characteristic.⁵ Experiments with Al microbridges²⁴ showed that pure aluminum samples of at least several tens of micrometers in length could be considered as ‘‘single-PS-center activated.’’ However, the resistive anomaly for Al should disappear on lengths more than several micrometers (Fig. 5), which is in a reasonable agreement with the experiment.⁷

IV. DISCUSSION

The present theoretical considerations being based on the thermal fluctuation model³ differ significantly in the procedure of ‘‘linkage’’ of the instantaneous voltage $V(t')$ across the sample with the corresponding time-averaged value $\langle V \rangle$. In Ref. 3 it was assumed that the average PS activation rate Γ_T should be balanced through the Josephson relation by the time-averaged voltage $\Gamma_T = 2e\langle V \rangle / \hbar$. This assumption is useful when the distance between potential probes is large compared to the nonequilibrium region attributed to each PS center, $|x_L - x_R| \gg \Lambda$. Thus, the actual dynamics of PS events is taken into consideration in a ‘‘statistical’’ way. However, for mesoscopic scales we must perform the time averaging more definitely. Introducing the $\tau_{Q^*}\Gamma_T$ weight is the easiest and the most straightforward possibility.

It should be mentioned that utilizing the τ_{Q^*} as a characteristic time for relaxation of charge imbalance by pulse injection of quasiparticles is still questionable. For steady-state conditions the validity of τ_{Q^*} applicability was confirmed undoubtedly,^{1,2} while for discrete PS events the experiments⁵ give both temperature-dependent and constant values for the corresponding relaxation time, working in favor of τ_{Q^*} and τ_E , respectively. As the thermal activation rate Γ_T is slightly affected by external magnetic field, τ_E is a material constant, and τ_{Q^*} is very sensitive to magnetic field pair breaking (Fig. 4), the comparison of the present model with experi-

ments in a magnetic field may bring additional clearness to the problem.

The key question of the present paper is how the resistance of a superconductor in the resistive state could exceed the corresponding normal-state value. Intuitively the resistivity per unit length ρ_q associated with nonequilibrium quasiparticles could be less or equal than the ρ_N . Consequently, no tricks with time averaging could obtain the situation $\langle R \rangle / R_{\text{normal}} > 1$. However, the expression for the effective resistance ratio Eq. (15) also contains the $\sim \Lambda / |x_L - x_R|$ term, which may be much greater than unity for mesoscopic samples. The physical significance of the last statement is the fact that in the resistive state of superconductors the amplitude of the chemical potential jump eU , Eqs. (12), (13), is set by the quasiparticles from the total nonequilibrium region $\sim 2\Lambda\rho_q$, while in the normal state the corresponding value is proportional to $\sim \rho_N|x_L - x_R|$. The usual approximation of equality of ρ_q and ρ_N indirectly assumes that the quasiparticle excitation spectrum differs from the one in normal state mainly by the existence of the energy gap and could be described by the ‘‘same’’ density of states $N(0)$ on the Fermi level and the distribution function $f = f_0 + \delta f$. The last statement brings us again to the requirement of the local equilibrium approximation in order that the quasiparticles could be described by a definite value of the chemical potential μ_q . However, the thermalization process is maintained by phonon emission and is characterized by the relaxation time τ_E .² For sufficiently intensive pumping of quasiparticles $\Gamma_T \gg \tau_E^{-1}$ the present model may not be valid. Fortunately, for most type-I superconductors Pb, Sn, In, and Al of mesoscopic dimensions the above nonequality never holds, while for Zn in the experimentally convenient range of bias currents the local equilibrium approximation may be violated and the application of the present model needs further justification. It would be very interesting to perform experiments on various materials with different types of probes. The present model qualitatively describes the existing experimental results on Al mesoscopic samples⁷⁻¹⁰ and the absence of any anomaly for In (Ref. 7) as indium is a short- τ_E material: $\Gamma_T \tau_Q \ll 1$. It would be useful to test the present theoretical considerations on Zn, probably setting the limits of applicability.

Unfortunately, at the present moment there are only few experimental works⁷⁻¹⁰ related to the present model. The two of them^{9,10} were performed on the multiple-connected samples (loops). The direct application of the present model to the ring geometry is questionable as there exist the parallel supercurrent channel due to the second arm of the loop. Figure 6 represents the comparison of the present model calculations with experimental results on Al wires.⁷ One should not be surprised that the experimental resistive transitions are much broader than the theoretical ones (Fig. 6). The present model deals with ideal 1D wires. For such homogeneous samples the calculated width of the resistive transition is about few mK and is comparable to the experimental results obtained on perfect whiskers.⁵ The actual sample prepared by a lift-off process⁷⁻¹⁰ is far from being considered an ideal homogeneous object. However, one can increase the calculated width of the resistive transition of such an inhomogeneous sample by introducing the random distribution of the local transition temperature T_c within the range ΔT_c .

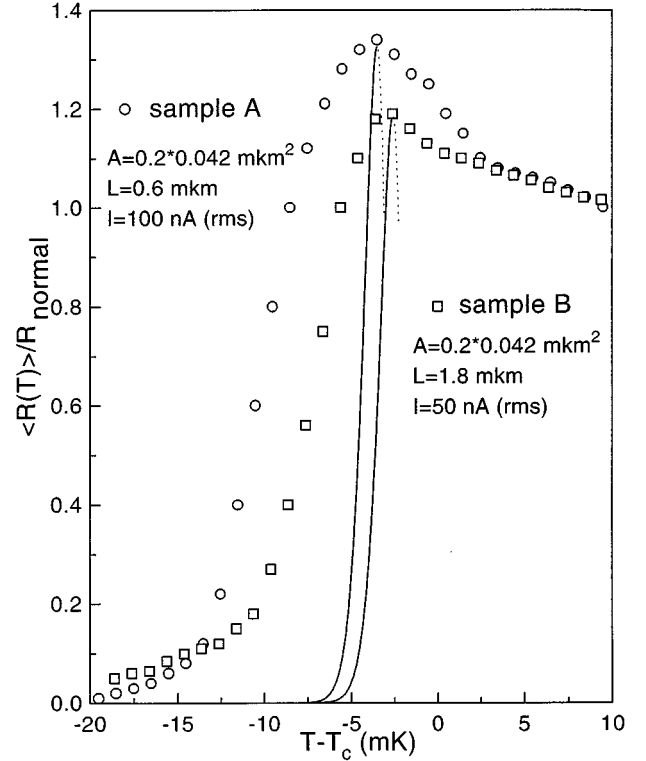


FIG. 6. Zero-field experimental resistive transition (\circ and \square) for mesoscopic Al wires. Data are taken from Ref. 7. Solid lines represent the present model calculations. It is assumed that the weakest link (PS center) is symmetrically referred to the superconducting voltage probes. The best fit is obtained using $T_c = 1.291$ K and 1.289 K, $I^{\text{dc}} = 122$ nA and 61 nA, and $\xi(0) = 157$ nm and 129 nm for samples A and B, respectively. For details see the text.

The main uncertainty in fitting the calculations to the experiment⁷ comes from the fact that in order to increase the signal-to-noise ratio the measurements were performed using the ac lock-in technique, while the present model is developed for the dc case. We found that the best fitting dc value I^{dc} is between the rms and the amplitude values of the experimentally used ac bias currents. As the current dependences of the model (Fig. 3) are much stronger than the length ones (Fig. 5), by fixing the effective dc bias current and utilizing the given sample geometry⁷ one can calculate the effective coherence length. The obtained values for $\xi(0)$ are in a reasonable agreement with the value 170 nm derived for the codeposited Al film.⁷ Slight deviations (see Fig. 6 caption) of $\xi(0)$ and T_c for the parts A and B could be easily understood as the samples were prepared from the nonoverlapping regions of the same wire.⁷

ACKNOWLEDGMENTS

The author wants to acknowledge Dr. Ya. G. Ponomarev and Dr. M. Yu. Kupriyanov for valuable discussions and careful reading of the manuscript. The work has been supported by the Russian Fund for Fundamental Research, Grant No. 95-02-04151-A, and by Grant No. NCX300 from the International Science Foundation and Russian Government.

- ¹J. Clarke, Phys. Rev. Lett. **28**, 1363 (1972).
- ²M. Tinkham and J. Clarke, Phys. Rev. Lett. **28**, 1366 (1972).
- ³J. S. Langer and V. Ambegaokar, Phys. Rev. **164**, 498 (1967).
- ⁴D. E. McCumber and B. I. Halperin, Phys. Rev. B **1**, 1054 (1970).
- ⁵See, for a review, R. Tidecks, *Current-Induced Nonequilibrium Phenomena in Quasi-One-Dimensional Superconductors* (Springer, New York, 1990).
- ⁶A. M. Kadin, L. N. Smith, and W. J. Skocpol, J. Low Temp. Phys. **38**, 497 (1980).
- ⁷P. Santhanam *et al.*, Phys. Rev. Lett. **66**, 2254 (1991).
- ⁸Y. K. Kwong *et al.*, Phys. Rev. B **44**, 462 (1991).
- ⁹H. Vloeberghs *et al.*, Phys. Rev. Lett. **69**, 1268 (1992).
- ¹⁰J.-J. Kim *et al.*, Physica B **194-196**, 1035 (1994); **194-196**, 1647 (1994).
- ¹¹G. J. Dolan and L. D. Jackel, Phys. Rev. Lett. **39**, 1628 (1977);
W. J. Skocpol and L. D. Jackel, Physica B **108**, 1021 (1981).
- ¹²N. Giordano, Phys. Rev. B **41**, 6350 (1990).
- ¹³V. V. Moshchalkov *et al.*, Phys. Rev. B **49**, 15 412 (1994).
- ¹⁴J. E. Lukens, R. J. Warburton, and W. W. Webb, Phys. Rev. Lett. **25**, 1180 (1970).
- ¹⁵R. S. Newbower, M. R. Beasley, and M. Tinkham, Phys. Rev. B **5**, 864 (1972).
- ¹⁶W. J. Skocpol, M. R. Beasley, and M. Tinkham, J. Low Temp. Phys. **16**, 145 (1974).
- ¹⁷A. Schmid and G. Schon, J. Low Temp. Phys. **20**, 207 (1975).
- ¹⁸K. Maki, in *Superconductivity*, edited by R. D. Parks (Marcel Dekker, New York, 1969).
- ¹⁹T. R. Lemberger and J. Clarke, Phys. Rev. B **23**, 1100 (1981).
- ²⁰M. Tinkham, *Introduction to Superconductivity* (McGraw-Hill, New York, 1975).
- ²¹M. Stuiyinga, J. E. Mooij, and T. M. Klapwijk, J. Low Temp. Phys. **46**, 555 (1982).
- ²²A. M. Kadin, W. J. Skocpol, and M. Tinkham, J. Low Temp. Phys. **33**, 481 (1978).
- ²³P. Santhanam, C. P. Umbach, and C. C. Chi, Phys. Rev. B **40**, 11 392 (1989).
- ²⁴T. M. Klapwijk, M. Sepers, and J. E. Mooij, J. Low Temp. Phys. **27**, 801 (1977).